Elements of a Scientific Paper:
Writing a Compelling Abstract and Introduction

WRITING SUCCESSFUL MANUSCRIPTS FOR PHYSICAL REVIEW LETTERS

Saad E. Hebboul *

The American Physical Society, Ridge, NY

PART 1 of 2

* *Email: hebboul@aps.org*

To see full lecture, go to:
https://ws.engr.illinois.edu/sitemanager/getfile.asp?id=2944

Key Steps to Writing an Accessible Paper

(1). Identify and ***write for*** your audience (e.g., expert, general, etc.) – this will govern the level of the presentation, i.e., the words you use, the number of topics you cover, the figures and results you present

(2). Develop a coherent and concise "story" to present your data – sketch out an abstract and introduction

(3). Sketch out a logical and concise outline for presenting the "story" of your scientific results – create an outline!

(4). Write simply and concisely, following the outline of your "story", avoiding disruptions to the flow of your narrative

The Mechanical Structure of a *Physical Review Letter*

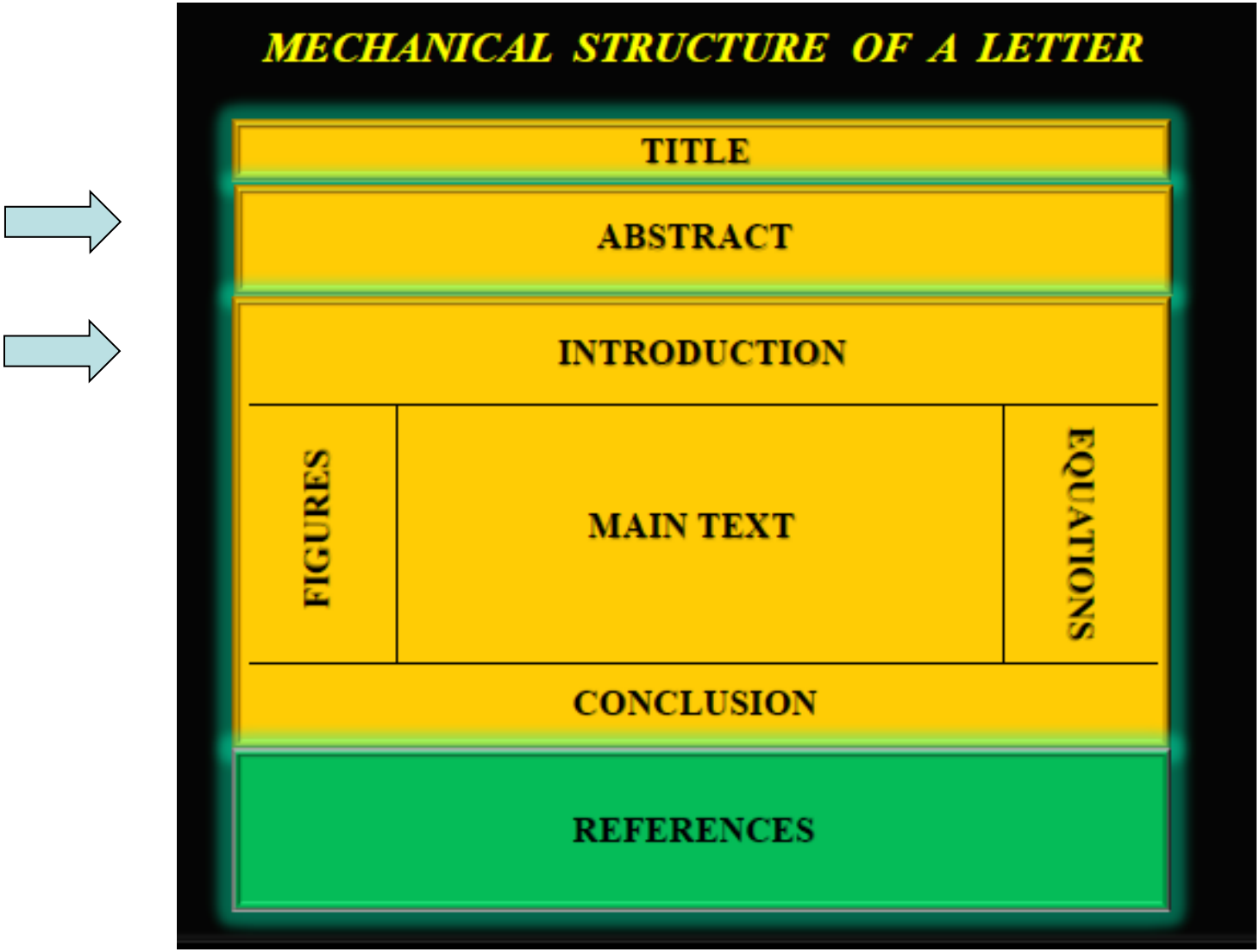

Editor Saad Hebboul:
https://ws.engr.illinois.edu/sitemanager/getfile.asp?id=2944

Effective Scientific Abstracts

One of the first, and most important, things you will need to write as a grad student, postdoc, etc., is a scientific abstract!

Scientific abstracts* are written for:

- Conferences and workshops (e.g., APS April and March Meetings) you plan to attend
- Proposals you will write
- Journal articles you will write
- Prelim papers and theses you will write
- Seminars and colloquia you will give

*Also very similar to project summaries, whitepapers, research statements, etc., you may write in the future

Effective Scientific Abstracts

The abstract provides an overview of the motivations, methods, and results in your paper or presentation

One function of an abstract is to “advertise” your paper or presentation:

Because the abstract is generally the first thing the reader will see, the quality of your abstract helps determine whether the reader will read your paper or attend your talk!

Because abstracts are often published or available online, abstracts also function as a permanent record of your paper or presentation

Published abstract booklets
Talk abstracts posted on-line
Paper abstracts available on INSPEC, SCOPUS, WOS,…

Developing a Coherent Story You Want to Tell About Your Results: **the Scientific Abstract**

The abstract is the most succinct expression of **what** you did, **why** you did it, and **what** was important about what you did.

Consequently, after conducting your research, ***sketching out a draft abstract*** will help you organize your thoughts so you can identify whether you have a coherent story that you can support with scientific evidence.

This process can help you tell if you're ready to write a paper and what the focus of your paper is.

Elements of a Scientific Abstract

Why is an abstract useful in this regard? The abstract should contain (in this order):

1. A brief statement of the motivations and/or issues associated with the research
2. A short description of the methods used
3. A summary of the key results obtained
4. A statement of the implications of the key results

So, the abstract contains all the essential elements of your paper, which is why starting with an abstract allows you to construct the coherent story you want to tell about your research!

Example Scientific Abstract

PRL 107, 117401 (2011) PHYSICAL REVIEW LETTERS week ending 9 SEPTEMBER 2011

Optical Response of Relativistic Electrons in the Polar BiTeI Semiconductor

J. S. Lee,[1,*] G. A. H. Schober,[2,3] M. S. Bahramy,[4] H. Murakawa,[5] Y. Onose,[2,5] R. Arita,[2,4] N. Nagaosa,[2,4] and Y. Tokura[1,2,4,5]

The transitions between the spin-split bands by spin-orbit interaction are relevant to many novel phenomena such as the resonant dynamical magnetoelectric effect and the spin Hall effect. We perform optical spectroscopy measurements combined with first-principles calculations to study these transitions in the recently discovered giant bulk Rashba spin-splitting system BiTeI. Several novel features are observed in the optical spectra of the material including a sharp edge singularity due to the reduced dimensionality of the joint density of states and a systematic doping dependence of the intraband transitions between the Rashba-split branches. These confirm the bulk nature of the Rashba-type splitting in BiTeI and manifest the relativistic nature of the electron dynamics in a solid.

Example Scientific Abstract

PRL 107, 117401 (2011) PHYSICAL REVIEW LETTERS week ending 9 SEPTEMBER 2011

Optical Response of Relativistic Electrons in the Polar BiTeI Semiconductor

J. S. Lee,[1,*] G. A. H. Schober,[2,3] M. S. Bahramy,[4] H. Murakawa,[5] Y. Onose,[2,5] R. Arita,[2,4] N. Nagaosa,[2,4] and Y. Tokura[1,2,4,5]

Motivation

The transitions between the spin-split bands by spin-orbit interaction are relevant to many novel phenomena such as the resonant dynamical magnetoelectric effect and the spin Hall effect. We perform optical spectroscopy measurements combined with first-principles calculations to study these transitions in the recently discovered giant bulk Rashba spin-splitting system BiTeI. Several novel features are observed in the optical spectra of the material including a sharp edge singularity due to the reduced dimensionality of the joint density of states and a systematic doping dependence of the intraband transitions between the Rashba-split branches. These confirm the bulk nature of the Rashba-type splitting in BiTeI and manifest the relativistic nature of the electron dynamics in a solid.

Example Scientific Abstract

PRL 107, 117401 (2011) PHYSICAL REVIEW LETTERS week ending 9 SEPTEMBER 2011

Optical Response of Relativistic Electrons in the Polar BiTeI Semiconductor

J. S. Lee,[1,*] G. A. H. Schober,[2,3] M. S. Bahramy,[4] H. Murakawa,[5] Y. Onose,[2,5] R. Arita,[2,4] N. Nagaosa,[2,4] and Y. Tokura[1,2,4,5]

Methods used

The transitions between the spin-split bands by spin-orbit interaction are relevant to many novel phenomena such as the resonant dynamical magnetoelectric effect and the spin Hall effect. We perform optical spectroscopy measurements combined with first-principles calculations to study these transitions in the recently discovered giant bulk Rashba spin-splitting system BiTeI. Several novel features are observed in the optical spectra of the material including a sharp edge singularity due to the reduced dimensionality of the joint density of states and a systematic doping dependence of the intraband transitions between the Rashba-split branches. These confirm the bulk nature of the Rashba-type splitting in BiTeI and manifest the relativistic nature of the electron dynamics in a solid.

Example Scientific Abstract

PRL 107, 117401 (2011) PHYSICAL REVIEW LETTERS week ending 9 SEPTEMBER 2011

Optical Response of Relativistic Electrons in the Polar BiTeI Semiconductor

J. S. Lee,[1,*] G. A. H. Schober,[2,3] M. S. Bahramy,[4] H. Murakawa,[5] Y. Onose,[2,5] R. Arita,[2,4] N. Nagaosa,[2,4] and Y. Tokura[1,2,4,5]

The transitions between the spin-split bands by spin-orbit interaction are relevant to many novel phenomena such as the resonant dynamical magnetoelectric effect and the spin Hall effect. We perform optical spectroscopy measurements combined with first-principles calculations to study these transitions in the recently discovered giant bulk Rashba spin-splitting system BiTeI. Several novel features are observed in the optical spectra of the material including a sharp edge singularity due to the reduced dimensionality of the joint density of states and a systematic doping dependence of the intraband transitions between the Rashba-split branches. These confirm the bulk nature of the Rashba-type splitting in BiTeI and manifest the relativistic nature of the electron dynamics in a solid.

Brief summary of key results

Example Scientific Abstract

PRL 107, 117401 (2011) PHYSICAL REVIEW LETTERS week ending 9 SEPTEMBER 2011

Optical Response of Relativistic Electrons in the Polar BiTeI Semiconductor

J. S. Lee,[1,*] G. A. H. Schober,[2,3] M. S. Bahramy,[4] H. Murakawa,[5] Y. Onose,[2,5] R. Arita,[2,4] N. Nagaosa,[2,4] and Y. Tokura[1,2,4,5]

The transitions between the spin-split bands by spin-orbit interaction are relevant to many novel phenomena such as the resonant dynamical magnetoelectric effect and the spin Hall effect. We perform optical spectroscopy measurements combined with first-principles calculations to study these transitions in the recently discovered giant bulk Rashba spin-splitting system BiTeI. Several novel features are observed in the optical spectra of the material including a sharp edge singularity due to the reduced dimensionality of the joint density of states and a systematic doping dependence of the intraband transitions between the Rashba-split branches. These confirm the bulk nature of the Rashba-type splitting in BiTeI and manifest the relativistic nature of the electron dynamics in a solid.

Brief statement of implications of results

Celia Elliott's Abstract Recipe

Generate your abstract by answering the following questions, in one or two sentences each:

- What problem did you study and why is it important?
- What methods did you use?
- What were your principal results?
- What conclusions can you draw from your results, or what are the implications of your results?

Make your sentences as *specific* and *quantitative* as possible!!

More Advice from Celia

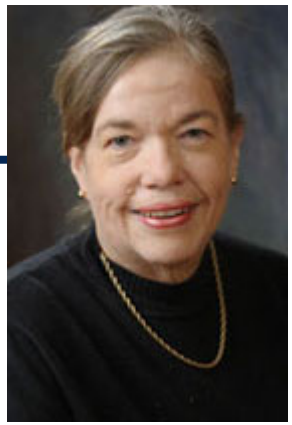

Control the length of your abstract by controlling the length of your answers to the four questions, NOT by omitting any of the answers:

Short abstract (~100 word, e.g., *Phys. Rev. Lett.* abstract):

one-sentence answers

Longer abstract (~200 word, e.g., *Phys. Review* abstract):

2-3 sentence answers

One-page abstract (e.g., proposal project summary):

one paragraph answers

Additional Advice on the Abstract

Your scientific abstract:

Should involve well-developed, grammatical sentences and paragraphs

- Don't take grammatical shortcuts just because it's an abstract!

Should be understandable by a non-expert audience

- e.g., avoid using specialized terms

Should be able to stand alone from the paper

- Don't refer to figures in paper
- Don't include references
- Define all acronyms

Should NOT contain complex equations, figures, tables

Should NOT contain information NOT in the paper

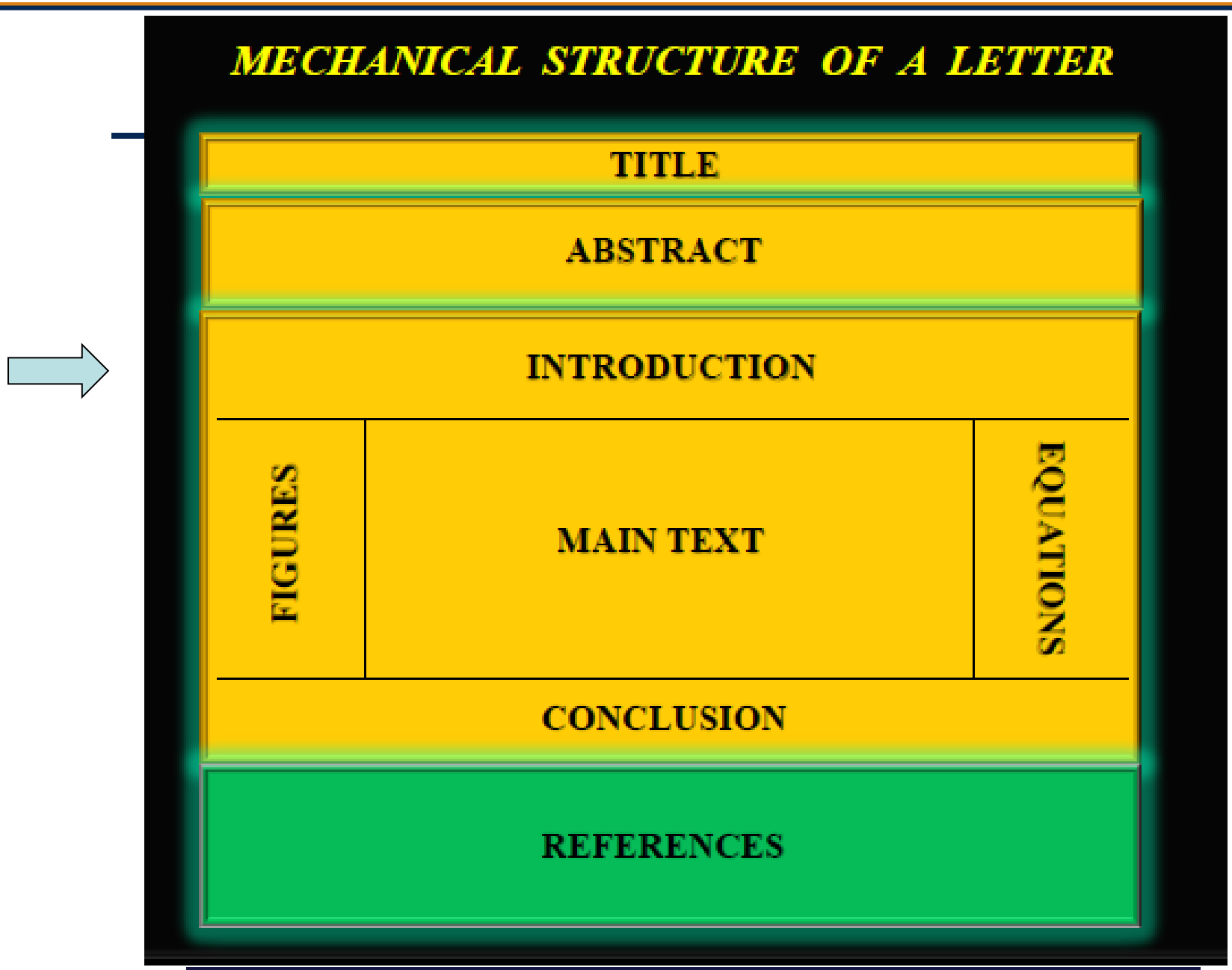

Editor Saad Hebboul: http://physics.illinois.edu/careers-seminar/UIUC_PRL_Workshop_Hebboul_Pt1.pdf

The Introduction: Most Important Part of an Accessible Paper

An accessible introduction provides:

-- The motivation and importance of the research

-- Background information a non-expert scientific audience needs to understand the research

-- A justification of why the research is needed

-- A preview of the key results of the paper

Note that, like the abstract, the introduction provides all the crucial elements of the story you want to tell.

As discussed last week, an accessible and compelling introduction improves the chances for your paper to (i) pass editorial review; (ii) be approved for publication by referees; and (iii) be understood and cited by your readers.

The Typical Structure of a Scientific Introduction

INTRODUCTION

FOR LETTERS

Consists of three crucial parts …

BACKGROUND or SURVEY

PHYSICAL MOTIVATION

IN THIS LETTER (Contribution)

… that form a single coherent story.

Editor Saad Hebboul: http://physics.illinois.edu/careers-seminar/UIUC_PRL_Workshop_Hebboul_Pt1.pdf

Information in the Introduction is Generally Organized in an "Inverted Pyramid" Structure

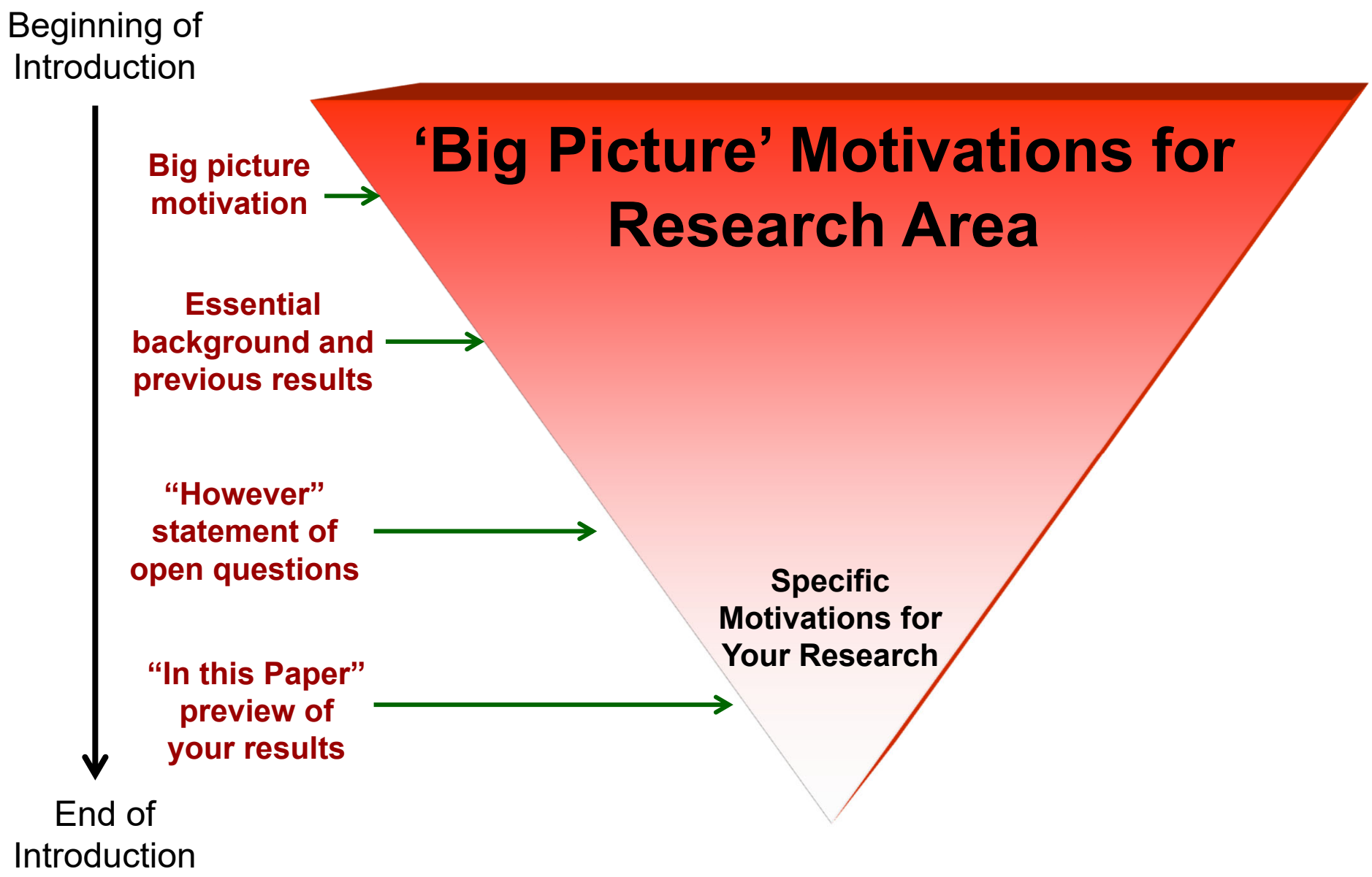

Observation of Spin Correlation in $t\bar{t}$ Events from pp Collisions at $\sqrt{s} = 7$ TeV Using the ATLAS Detector

"Big Picture" opening ⟶

The top quark was discovered in 1995 [1,2] at the Tevatron proton-antiproton collider. The lifetime of the top quark is at least an order of magnitude shorter than the time scale for strong interactions, implying that the top quark decays before hadronization [3–7]. Therefore the spin of the top quark at production is transferred to its decay products and can be measured directly via their angular distributions [4]. While the polarization of t and $\bar{t}$ quarks in a hadronically produced $t\bar{t}$ sample is predicted to be very small, their spins are predicted to be correlated [8–10]. In this Letter the hypothesis that the correlation of the spin of top and antitop quarks in $t\bar{t}$ events is as expected in the standard model (SM), as opposed to the hypothesis that they are uncorrelated, is tested. This tests the precise predictions of $t\bar{t}$ pair production and of top quark decay, which is expected to occur before its spin is flipped by the strong interaction [9–13]. Many scenarios of new physics beyond the SM predict different spin correlations while keeping the $t\bar{t}$ production cross section within experimental and theoretical bounds [14–18]. For example, the spin correlation measured in this Letter may differ from the SM if the $t\bar{t}$ pairs were produced via the exchange of a virtual heavy scalar Higgs boson [19] or if the top quark decayed into a scalar charged Higgs boson and a b quark ($t \to H^+ b$) [20].

At the LHC $t\bar{t}$ production occurs mostly through the $gg \to t\bar{t}$ channel. At low $t\bar{t}$ invariant mass it is dominated by the fusion of like-helicity gluon pairs which produce top quarks in the left-left or right-right helicity configurations [13]. When these decay via $t\bar{t} \to W^+W^-b\bar{b} \to l^+\nu l^-\bar{\nu}b\bar{b}$ they produce charged leptons which possess correlations in

Observation of Spin Correlation in $t\bar{t}$ Events from pp Collisions at $\sqrt{s} = 7$ TeV Using the ATLAS Detector

Background info; narrowing of focus to specific topic →

The top quark was discovered in 1995 [1,2] at the Tevatron proton-antiproton collider. The lifetime of the top quark is at least an order of magnitude shorter than the time scale for strong interactions, implying that the top quark decays before hadronization [3–7]. Therefore the spin of the top quark at production is transferred to its decay products and can be measured directly via their angular distributions [4]. While the polarization of t and $\bar{t}$ quarks in a hadronically produced $t\bar{t}$ sample is predicted to be very small, their spins are predicted to be correlated [8–10]. In this Letter the hypothesis that the correlation of the spin of top and antitop quarks in $t\bar{t}$ events is as expected in the standard model (SM), as opposed to the hypothesis that they are uncorrelated, is tested. This tests the precise predictions of $t\bar{t}$ pair production and of top quark decay, which is expected to occur before its spin is flipped by the strong interaction [9–13]. Many scenarios of new physics beyond the SM predict different spin correlations while keeping the $t\bar{t}$ production cross section within experimental and theoretical bounds [14–18]. For example, the spin correlation measured in this Letter may differ from the SM if the $t\bar{t}$ pairs were produced via the exchange of a virtual heavy scalar Higgs boson [19] or if the top quark decayed into a scalar charged Higgs boson and a b quark ($t \to H^+ b$) [20].

At the LHC $t\bar{t}$ production occurs mostly through the $gg \to t\bar{t}$ channel. At low $t\bar{t}$ invariant mass it is dominated by the fusion of like-helicity gluon pairs which produce top quarks in the left-left or right-right helicity configurations [13]. When these decay via $t\bar{t} \to W^+W^-b\bar{b} \to l^+\nu l^-\bar{\nu}b\bar{b}$ they produce charged leptons which possess correlations in

Observation of Spin Correlation in $t\bar{t}$ Events from pp Collisions at $\sqrt{s} = 7$ TeV Using the ATLAS Detector

Motivation for paper (or "straw man" statement): why the research in this paper is necessary →

The top quark was discovered in 1995 [1,2] at the Tevatron proton-antiproton collider. The lifetime of the top quark is at least an order of magnitude shorter than the time scale for strong interactions, implying that the top quark decays before hadronization [3–7]. Therefore the spin of the top quark at production is transferred to its decay products and can be measured directly via their angular distributions [4]. While the polarization of t and $\bar{t}$ quarks in a hadronically produced $t\bar{t}$ sample is predicted to be very small, their spins are predicted to be correlated [8–10]. In this Letter the hypothesis that the correlation of the spin of top and antitop quarks in $t\bar{t}$ events is as expected in the standard model (SM), as opposed to the hypothesis that they are uncorrelated, is tested. This tests the precise predictions of $t\bar{t}$ pair production and of top quark decay, which is expected to occur before its spin is flipped by the strong interaction [9–13]. Many scenarios of new physics beyond the SM predict different spin correlations while keeping the $t\bar{t}$ production cross section within experimental and theoretical bounds [14–18]. For example, the spin correlation measured in this Letter may differ from the SM if the $t\bar{t}$ pairs were produced via the exchange of a virtual heavy scalar Higgs boson [19] or if the top quark decayed into a scalar charged Higgs boson and a b quark ($t \to H^+ b$) [20].

At the LHC $t\bar{t}$ production occurs mostly through the $gg \to t\bar{t}$ channel. At low $t\bar{t}$ invariant mass it is dominated by the fusion of like-helicity gluon pairs which produce top quarks in the left-left or right-right helicity configurations [13]. When these decay via $t\bar{t} \to W^+W^-b\bar{b} \to l^+\nu l^-\bar{\nu}b\bar{b}$ they produce charged leptons which possess correlations in

Observation of Spin Correlation in $t\bar{t}$ Events from pp Collisions at $\sqrt{s} = 7$ TeV Using the ATLAS Detector

Preview of key results in this paper →

The top quark was discovered in 1995 [1,2] at the Tevatron proton-antiproton collider. The lifetime of the top quark is at least an order of magnitude shorter than the time scale for strong interactions, implying that the top quark decays before hadronization [3–7]. Therefore the spin of the top quark at production is transferred to its decay products and can be measured directly via their angular distributions [4]. While the polarization of t and $\bar{t}$ quarks in a hadronically produced $t\bar{t}$ sample is predicted to be very small, their spins are predicted to be correlated [8–10]. In this Letter the hypothesis that the correlation of the spin of top and antitop quarks in $t\bar{t}$ events is as expected in the standard model (SM), as opposed to the hypothesis that they are uncorrelated, is tested. This tests the precise predictions of $t\bar{t}$ pair production and of top quark decay, which is expected to occur before its spin is flipped by the strong interaction [9–13]. Many scenarios of new physics beyond the SM predict different spin correlations while keeping the $t\bar{t}$ production cross section within experimental and theoretical bounds [14–18]. For example, the spin correlation measured in this Letter may differ from the SM if the $t\bar{t}$ pairs were produced via the exchange of a virtual heavy scalar Higgs boson [19] or if the top quark decayed into a scalar charged Higgs boson and a b quark ($t \to H^+ b$) [20].

At the LHC $t\bar{t}$ production occurs mostly through the $gg \to t\bar{t}$ channel. At low $t\bar{t}$ invariant mass it is dominated by the fusion of like-helicity gluon pairs which produce top quarks in the left-left or right-right helicity configurations [13]. When these decay via $t\bar{t} \to W^+W^-b\bar{b} \to l^+\nu l^-\bar{\nu}b\bar{b}$ they produce charged leptons which possess correlations in

Pseudospin-Resolved Transport Spectroscopy of the Kondo Effect in a Double Quantum Dot

S. Amasha,[1] A. J. Keller,[1] I. G. Rau,[2,*] A. Carmi,[3] J. A. Katine,[4] Hadas Shtrikman,[3] Y. Oreg,[3] and D. Goldhaber-Gordon[1,3,†]

The Kondo effect is one of the paradigms of correlated electron physics [1]. It describes how itinerant electrons with a degenerate degree of freedom screen a localized state with the same degeneracy. Typically, the relevant degeneracy is spin: a localized electron is transitioned between degenerate spin states by spin-flip scattering with conduction electrons. Correlations are established between the localized and conduction electrons, with a many-body spin singlet resulting at low temperatures. This Kondo screening causes a resonance in the local density of states (LDOS) at the Fermi energy, which manifests itself in nanostructures as a zero-bias peak in the conductance [2]. While Kondo physics is usually associated with spin, nanostructures allow the realization of the Kondo effect based on orbital degeneracy [3–7]. The advantage to using an orbital degeneracy is its potential to realize a fully tunable state-resolved probe of Kondo physics that does not perturb the Kondo correlations, which is not possible in spin-based Kondo systems.

Spin-resolved transport measurements in nanostructures have been achieved using ferromagnetic contacts, leading to spin-dependent tunnel rates [8–10]. Unfortunately, these spin-dependent rates also affect Kondo physics [11–14]; moreover, the rates are fixed by the contact design and cannot be tuned. Another approach has been to use a quantum point contact as a spin polarizer [15] to build up a nonequilibrium distribution, with a spin-dependent Fermi energy [16]. However, this technique requires a magnetic field that breaks the spin degeneracy necessary for the Kondo effect.

We instead realize a tunable state-resolved probe of the Kondo effect using an orbital degeneracy of a double energy for an electron to be in dot 1 is the same as that for being in dot 2. These orbital states can be coherently manipulated as a two-level "pseudospin" system [19,20]. The advantage of studying a Kondo effect based on pseudospin degeneracy is that by controlling and measuring each of the dots individually, we can characterize the conductance of each pseudospin component [21–25].

In this Letter, we report pseudospin-resolved transport spectroscopy of the Kondo effect based on an orbital degeneracy in a DQD. We first demonstrate spectroscopy of the DQD analogous to standard transport spectroscopy in a single dot, and we use this to observe the zero-bias peak that is the hallmark of Kondo physics. In standard spectroscopy of spin Kondo, a magnetic field splits the Kondo peak so that the conductance at zero bias is suppressed and the Kondo peaks occur at positive and negative bias. In contrast, pseudospin-resolved spectroscopy of the orbital Kondo effect in a pseudomagnetic field shows a peak at only one sign of the bias, corresponding to the pseudospin state we are observing. Finally, we demonstrate that a single, consistent Kondo temperature can be defined for the entire DQD system.

We measure a laterally gated DQD fabricated from an epitaxially grown AlGaAs/GaAs heterostructure hosting a two-dimensional electron gas with a density of 2×10^{11} cm^{-2} and a mobility of 2×10^{6} cm^2/V s. We apply negative voltages to metallic surface gates (inset of Fig. 1) to form two capacitively coupled quantum dots with negligible interdot tunneling [26]. The gates W1L and W1U control the tunneling rates between dot 1 and its source and drain leads $\Gamma_{S1}/\hbar$ and $\Gamma_{D1}/\hbar$, respectively. We define $\Gamma_1 =$

"Big Picture" opening →

The Kondo effect is one of the paradigms of correlated electron physics [1]. It describes how itinerant electrons with a degenerate degree of freedom screen a localized state with the same degeneracy. Typically, the relevant degeneracy is spin: a localized electron is transitioned between degenerate spin states by spin-flip scattering with conduction electrons. Correlations are established between the localized and conduction electrons, with a many-body spin singlet resulting at low temperatures. This Kondo screening causes a resonance in the local density of states (LDOS) at the Fermi energy, which manifests itself in nanostructures as a zero-bias peak in the conductance [2]. While Kondo physics is usually associated with spin, nanostructures allow the realization of the Kondo effect based on orbital degeneracy [3–7]. The advantage to using an orbital degeneracy is its potential to realize a fully tunable state-resolved probe of Kondo physics that does not perturb the Kondo correlations, which is not possible in spin-based Kondo systems.

Spin-resolved transport measurements in nanostructures have been achieved using ferromagnetic contacts, leading to spin-dependent tunnel rates [8–10]. Unfortunately, these spin-dependent rates also affect Kondo physics [11–14]; moreover, the rates are fixed by the contact design and cannot be tuned. Another approach has been to use a quantum point contact as a spin polarizer [15] to build up a nonequilibrium distribution, with a spin-dependent Fermi energy [16]. However, this technique requires a magnetic field that breaks the spin degeneracy necessary for the Kondo effect.

We instead realize a tunable state-resolved probe of the Kondo effect using an orbital degeneracy of a double quantum dot (DQD) [17,18], which occurs when the

Background info; narrowing of focus to specific topic →

The Kondo effect is one of the paradigms of correlated electron physics [1]. It describes how itinerant electrons with a degenerate degree of freedom screen a localized state with the same degeneracy. Typically, the relevant degeneracy is spin: a localized electron is transitioned between degenerate spin states by spin-flip scattering with conduction electrons. Correlations are established between the localized and conduction electrons, with a many-body spin singlet resulting at low temperatures. This Kondo screening causes a resonance in the local density of states (LDOS) at the Fermi energy, which manifests itself in nanostructures as a zero-bias peak in the conductance [2]. While Kondo physics is usually associated with spin, nanostructures allow the realization of the Kondo effect based on orbital degeneracy [3–7]. The advantage to using an orbital degeneracy is its potential to realize a fully tunable state-resolved probe of Kondo physics that does not perturb the Kondo correlations, which is not possible in spin-based Kondo systems.

Spin-resolved transport measurements in nanostructures have been achieved using ferromagnetic contacts, leading to spin-dependent tunnel rates [8–10]. Unfortunately, these spin-dependent rates also affect Kondo physics [11–14]; moreover, the rates are fixed by the contact design and cannot be tuned. Another approach has been to use a quantum point contact as a spin polarizer [15] to build up a nonequilibrium distribution, with a spin-dependent Fermi energy [16]. However, this technique requires a magnetic field that breaks the spin degeneracy necessary for the Kondo effect.

We instead realize a tunable state-resolved probe of the Kondo effect using an orbital degeneracy of a double quantum dot (DQD) [17,18], which occurs when the

The Kondo effect is one of the paradigms of correlated electron physics [1]. It describes how itinerant electrons with a degenerate degree of freedom screen a localized state with the same degeneracy. Typically, the relevant degeneracy is spin: a localized electron is transitioned between degenerate spin states by spin-flip scattering with conduction electrons. Correlations are established between the localized and conduction electrons, with a many-body spin singlet resulting at low temperatures. This Kondo screening causes a resonance in the local density of states (LDOS) at the Fermi energy, which manifests itself in nanostructures as a zero-bias peak in the conductance [2]. While Kondo physics is usually associated with spin, nanostructures allow the realization of the Kondo effect based on orbital degeneracy [3–7]. The advantage to using an orbital degeneracy is its potential to realize a fully tunable state-resolved probe of Kondo physics that does not perturb the Kondo correlations, which is not possible in spin-based Kondo systems.

Motivation for paper (or "straw man" statement): why the research in this paper is necessary →

Spin-resolved transport measurements in nanostructures have been achieved using ferromagnetic contacts, leading to spin-dependent tunnel rates [8–10]. Unfortunately, these spin-dependent rates also affect Kondo physics [11–14]; moreover, the rates are fixed by the contact design and cannot be tuned. Another approach has been to use a quantum point contact as a spin polarizer [15] to build up a nonequilibrium distribution, with a spin-dependent Fermi energy [16]. However, this technique requires a magnetic field that breaks the spin degeneracy necessary for the Kondo effect.

We instead realize a tunable state-resolved probe of the Kondo effect using an orbital degeneracy of a double quantum dot (DQD) [17,18], which occurs when the

The Kondo effect is one of the paradigms of correlated electron physics [1]. It describes how itinerant electrons with a degenerate degree of freedom screen a localized state with the same degeneracy. Typically, the relevant degeneracy is spin: a localized electron is transitioned between degenerate spin states by spin-flip scattering with conduction electrons. Correlations are established between the localized and conduction electrons, with a many-body spin singlet resulting at low temperatures. This Kondo screening causes a resonance in the local density of states (LDOS) at the Fermi energy, which manifests itself in nanostructures as a zero-bias peak in the conductance [2]. While Kondo physics is usually associated with spin, nanostructures allow the realization of the Kondo effect based on orbital degeneracy [3–7]. The advantage to using an orbital degeneracy is its potential to realize a fully tunable state-resolved probe of Kondo physics that does not perturb the Kondo correlations, which is not possible in spin-based Kondo systems.

Spin-resolved transport measurements in nanostructures have been achieved using ferromagnetic contacts, leading to spin-dependent tunnel rates [8–10]. Unfortunately, these spin-dependent rates also affect Kondo physics [11–14]; moreover, the rates are fixed by the contact design and cannot be tuned. Another approach has been to use a quantum point contact as a spin polarizer [15] to build up a nonequilibrium distribution, with a spin-dependent Fermi energy [16]. However, this technique requires a magnetic field that breaks the spin degeneracy necessary for the Kondo effect.

We instead realize a tunable state-resolved probe of the Kondo effect using an orbital degeneracy of a double quantum dot (DQD) [17,18], which occurs when the energy for an electron to be in dot 1 is the same as that for being in dot 2. These orbital states can be coherently manipulated as a two-level "pseudospin" system [19,20]. The advantage of studying a Kondo effect based on pseudospin degeneracy is that by controlling and measuring each of the dots individually, we can characterize the conductance of each pseudospin component [21–25].

In this Letter, we report pseudospin-resolved transport spectroscopy of the Kondo effect based on an orbital degeneracy in a DQD. We first demonstrate spectroscopy of the DQD analogous to standard transport spectroscopy in a single dot, and we use this to observe the zero-bias peak that is the hallmark of Kondo physics. In standard spectroscopy of spin Kondo, a magnetic field splits the Kondo peak so that the conductance at zero bias is suppressed and the Kondo peaks occur at positive and negative bias. In contrast, pseudospin-resolved spectroscopy of the orbital Kondo effect in a pseudomagnetic field shows a peak at only one sign of the bias, corresponding to the pseudospin state we are observing. Finally, we demonstrate that a single, consistent Kondo temperature can be defined for the entire DQD system.

Preview of key results in this paper

Effects of Particle Shape on Growth Dynamics at Edges of Evaporating Drops of Colloidal Suspensions

Peter J. Yunker,[1] Matthew A. Lohr,[1] Tim Still,[1,2] Alexei Borodin,[3] D. J. Durian,[1] and A. G. Yodh[1]

Examples of surface and interfacial growth phenomena are diverse, ranging from the production of uniform coatings by vapor deposition of atoms onto a substrate [1], to burning paper wherein the combustion front roughens as it spreads [2,3], to bacterial colonies whose boundaries expand and fluctuate as bacteria replicate [4]. The morphology of the resulting interfaces is a property that affects the macroscopic responses of such systems, and it is therefore desirable to relate interface morphology to the microscopic rules that govern growth [1,5,6]. To this end, simulations have directly compared a broad range of growth processes [5,6] and have found, for example, that the random deposition of repulsive particles is a Poisson process, while the random deposition of "sticky" particles belongs to a different universality class that leads to different interface morphology.

Besides discrete models, theoretical investigation of this problem has centered around continuum growth equations (e.g., Ref. [7]). One interesting approach that unified a large set of discrete simulations is based on the so-called Kardar-Parisi-Zhang (KPZ) equation [6,8–12]. This nonlinear equation relates stochastic growth and interfacial growth fronts, lines, or surfaces to diffusion and local lateral correlations; its solutions are known and belong to the KPZ universality class [13–16]. The KPZ class presents a rare opportunity for connecting exact theoretical predictions about nonequilibrium growth phenomena with experiment. However, to date only a few members of the KPZ class have been experimentally identified [2–4,17]. This paucity of KPZ examples is due, in part, to the presence of quenched disorder and long-range interactions in experiment, as well as to limited statistics, which make broadly speaking, experimental confrontation of the microscopic rules explored by theory and simulation has been difficult.

In this contribution we demonstrate that the rich nonequilibrium physics of evaporating colloidal drops provides an attractive experimental system for study of such growth processes and for testing theory and simulation predictions. Specifically, we investigate the growth of particle deposits from the edges of evaporating colloidal drops. Particle deposition is observed by video microscopy at the single particle level. Aqueous suspensions of colloidal particles are allowed to evaporate on glass slides at constant temperature and humidity, and radial convective flows during evaporation carry particles from drop center to drop edge, where they accumulate [Fig. 1(a)] [18]. The resulting deposits of particles grow from the edge on the air-water interface in two dimensions, defining a deposition front, or growth line, that varies in space and time. Interestingly, these interfacial growth processes are strongly dependent on colloidal particle shape [19]. Three distinct growth processes were discovered in the evaporating colloidal suspensions by tuning particle shape-dependent capillary interactions and thus varying the microscopic rules of deposition. The substantial shape fluctuations of the growth line of spheres are readily explained via a Poisson-like deposition process; slightly anisotropic particles exhibit weaker fluctuations characteristic of KPZ class behavior, and very anisotropic ellipsoids exhibit behavior consistent with the KPZ class in the presence of quenched disorder [20–22].

Our experiments employ water drops containing a

"Big Picture" opening ⟶

Examples of surface and interfacial growth phenomena are diverse, ranging from the production of uniform coatings by vapor deposition of atoms onto a substrate [1], to burning paper wherein the combustion front roughens as it spreads [2,3], to bacterial colonies whose boundaries expand and fluctuate as bacteria replicate [4]. The morphology of the resulting interfaces is a property that affects the macroscopic responses of such systems, and it is therefore desirable to relate interface morphology to the microscopic rules that govern growth [1,5,6]. To this end, simulations have directly compared a broad range of growth processes [5,6] and have found, for example, that the random deposition of repulsive particles is a Poisson process, while the random deposition of "sticky" particles belongs to a different universality class that leads to different interface morphology.

Besides discrete models, theoretical investigation of this problem has centered around continuum growth equations (e.g., Ref. [7]). One interesting approach that unified a large set of discrete simulations is based on the so-called Kardar-Parisi-Zhang (KPZ) equation [6,8–12]. This nonlinear equation relates stochastic growth and interfacial growth fronts, lines, or surfaces to diffusion and local lateral correlations; its solutions are known and belong to the KPZ universality class [13–16]. The KPZ class presents a rare opportunity for connecting exact theoretical predictions about nonequilibrium growth phenomena with experiment. However, to date only a few members of the KPZ class have been experimentally identified [2–4,17]. This paucity of KPZ examples is due, in part, to the presence of quenched disorder and long-range interactions in experiment, as well as to limited statistics, which make growth process differences difficult to discern. In fact,

Background info; narrowing of focus to specific topic →

Examples of surface and interfacial growth phenomena are diverse, ranging from the production of uniform coatings by vapor deposition of atoms onto a substrate [1], to burning paper wherein the combustion front roughens as it spreads [2,3], to bacterial colonies whose boundaries expand and fluctuate as bacteria replicate [4]. The morphology of the resulting interfaces is a property that affects the macroscopic responses of such systems, and it is therefore desirable to relate interface morphology to the microscopic rules that govern growth [1,5,6]. To this end, simulations have directly compared a broad range of growth processes [5,6] and have found, for example, that the random deposition of repulsive particles is a Poisson process, while the random deposition of "sticky" particles belongs to a different universality class that leads to different interface morphology.

Besides discrete models, theoretical investigation of this problem has centered around continuum growth equations (e.g., Ref. [7]). One interesting approach that unified a large set of discrete simulations is based on the so-called Kardar-Parisi-Zhang (KPZ) equation [6,8–12]. This nonlinear equation relates stochastic growth and interfacial growth fronts, lines, or surfaces to diffusion and local lateral correlations; its solutions are known and belong to the KPZ universality class [13–16]. The KPZ class presents a rare opportunity for connecting exact theoretical predictions about nonequilibrium growth phenomena with experiment. However, to date only a few members of the KPZ class have been experimentally identified [2–4,17]. This paucity of KPZ examples is due, in part, to the presence of quenched disorder and long-range interactions in experiment, as well as to limited statistics, which make growth process differences difficult to discern. In fact,

Examples of surface and interfacial growth phenomena are diverse, ranging from the production of uniform coatings by vapor deposition of atoms onto a substrate [1], to burning paper wherein the combustion front roughens as it spreads [2,3], to bacterial colonies whose boundaries expand and fluctuate as bacteria replicate [4]. The morphology of the resulting interfaces is a property that affects the macroscopic responses of such systems, and it is therefore desirable to relate interface morphology to the microscopic rules that govern growth [1,5,6]. To this end, simulations have directly compared a broad range of growth processes [5,6] and have found, for example, that the random deposition of repulsive particles is a Poisson process, while the random deposition of "sticky" particles belongs to a different universality class that leads to different interface morphology.

Besides discrete models, theoretical investigation of this problem has centered around continuum growth equations (e.g., Ref. [7]). One interesting approach that unified a large set of discrete simulations is based on the so-called Kardar-Parisi-Zhang (KPZ) equation [6,8–12]. This nonlinear equation relates stochastic growth and interfacial growth fronts, lines, or surfaces to diffusion and local lateral correlations; its solutions are known and belong to the KPZ universality class [13–16]. The KPZ class presents a rare opportunity for connecting exact theoretical predictions about nonequilibrium growth phenomena with experiment. However, to date only a few members of the KPZ class have been experimentally identified [2–4,17]. This paucity of KPZ examples is due, in part, to the presence of quenched disorder and long-range interactions in experiment, as well as to limited statistics, which make growth process differences difficult to discern. In fact,

Motivation for paper (or "straw man" statement): why the research in this paper is necessary →

Preview of key results in this paper →

broadly speaking, experimental confrontation of the microscopic rules explored by theory and simulation has been difficult.

In this contribution we demonstrate that the rich nonequilibrium physics of evaporating colloidal drops provides an attractive experimental system for study of such growth processes and for testing theory and simulation predictions. Specifically, we investigate the growth of particle deposits from the edges of evaporating colloidal drops. Particle deposition is observed by video microscopy at the single particle level. Aqueous suspensions of colloidal particles are allowed to evaporate on glass slides at constant temperature and humidity, and radial convective flows during evaporation carry particles from drop center to drop edge, where they accumulate [Fig. 1(a)] [18]. The resulting deposits of particles grow from the edge on the air-water interface in two dimensions, defining a deposition front, or growth line, that varies in space and time. Interestingly, these interfacial growth processes are strongly dependent on colloidal particle shape [19]. Three distinct growth processes were discovered in the evaporating colloidal suspensions by tuning particle shape-dependent capillary interactions and thus varying the microscopic rules of deposition. The substantial shape fluctuations of the growth line of spheres are readily explained via a Poisson-like deposition process; slightly anisotropic particles exhibit weaker fluctuations characteristic of KPZ class behavior, and very anisotropic ellipsoids exhibit behavior consistent with the KPZ class in the presence of quenched disorder [20–22].

Our experiments employ water drops containing a suspension of polystyrene spheres (Invitrogen) stretched asymmetrically to different aspect ratios [19,23,24].

Laser cooling of a semiconductor by 40 kelvin

Jun Zhang[1]*, Dehui Li[1]*, Renjie Chen[1] & Qihua Xiong[1,2]

Nature **493**, 504 (2013)

Laser cooling of a semiconductor by 40 kelvin

Jun Zhang[1]*, Dehui Li[1]*, Renjie Chen[1] & Qihua Xiong[1,2]

Nature **493**, 504 (2013)

Optical irradiation accompanied by spontaneous anti-Stokes emission can lead to cooling of matter, in a phenomenon known as laser cooling, or optical refrigeration, which was proposed by Pringsheim in 1929[1]. In gaseous matter, an extremely low temperature can be obtained in diluted atomic gases by Doppler cooling[2], and laser cooling of ultradense gas has been demonstrated by collisional redistribution of radiation[3]. In solid-state materials, laser cooling is achieved by the annihilation of phonons, which are quanta of lattice vibrations, during anti-Stokes luminescence. Since the first experimental demonstration in glasses doped with rare-earth metals[4], considerable progress has been made, particularly in ytterbium-doped glasses or crystals: recently a record was set of cooling to about 110 kelvin from the ambient temperature, surpassing the thermoelectric Peltier cooler[5,6]. It would be interesting to realize laser cooling in semiconductors, in which excitonic resonances dominate[7–9], rather than in systems doped with rare-earth metals, where atomic resonances dominate. However, so far no net cooling in semiconductors has been achieved despite much experimental[10–12] and theoretical[7–9,13,14] work, mainly on group-III–V gallium arsenide quantum wells. Here we report a net cooling by about 40 kelvin in a semiconductor using group-II–VI cadmium sulphide nanoribbons, or nanobelts, starting from 290 kelvin. We use a pump laser with a wavelength of 514 nanometres, and obtain an estimated cooling efficiency of about 1.3 per cent and an estimated cooling power of 180 microwatts. At 100 kelvin, 532-nm pumping leads to a net cooling of about 15 kelvin with a cooling efficiency of about 2.0 per cent. We attribute the net laser cooling in cadmium sulphide nanobelts to strong coupling between excitons and longitudinal optical phonons (LOPs), which allows the resonant annihilation of multiple LOPs in luminescence up-conversion processes, high external quantum efficiency and negligible background absorption. Our findings suggest that, alternatively, group-II–VI semiconductors with strong exciton–LOP coupling could be harnessed to achieve laser cooling and open the way to optical refrigeration based on semiconductors.

Here v is the pump laser frequency, T is the absolute temperature of the sample, $\bar{\nu}_f(T)$ is the mean emission frequency and h is Planck's constant; η_{exe} is the external quantum efficiency, written as $\eta_{exe} = \eta_e W_{rad}/(\eta_e W_{rad} + W_{nr})$, where η_e is the luminescence extraction efficiency and W_{rad} and W_{nr} are respectively the radiative and non-radiative recombination rates; and $\eta_{abs} = [1 + \alpha_b/\alpha(v, T)]^{-1}$ is the absorption efficiency, quantifying the percentage of photons absorbed that are engaged in cooling, where α_b is the background absorption coefficient and $\alpha(v, T)$ is the semiconductor absorption coefficient. Net laser cooling requires $\eta_c(hv, T) > 0$, which might be achieved in three related ways: having a large energy difference $\Delta E = h\bar{\nu}_f(T) - hv$; having η_{exe} approach unity; and having η_{abs} approach unity through the minimization of the background absorption, α_b.

In the classical Pringsheim picture applied to solids, each cooling cycle removes $\Delta E = h\bar{\nu}_f(T) - hv \approx k_B T$ during the thermalization of cold electrons and holes, owing to absorption of various phonons. In GaAs, single LOP-assisted transitions in band-tail absorption (Urbach tail) have been proposed to facilitate laser cooling[20,21]. It has also been proposed that the band structure can be engineered, for example by introducing donor–acceptor pairs, which modifies the density of states and could lead to a larger ΔE, making the dependence on the other two factors (η_{exe} and η_{abs}) less important. However, experimentally that is difficult to achieve because the doping density and binding energies of both donors and acceptors have to be simultaneously optimized. We find that strong exciton–LOP coupling in II–VI semiconductors such as cadmium sulphide (CdS) can be harnessed to facilitate laser cooling by the annihilation of one or more LOPs, leading to the removal of several $k_B T$ units of heat in each cooling cycle.

Figure 1a shows the anti-Stokes photoluminescence spectra of a CdS nanobelt excited by a 532-nm laser (bottom) and a 514-nm laser (top) at 294 K at three different pumping powers. Strong anti-Stokes photoluminescence with a peak position of ~506 nm is identified, facilitated by resonant annihilation of multiple LOPs (one for the 514-nm laser and three for the 532-nm laser; $h\nu_{LO} \approx 37$ meV, or 300 cm^{-1}). We note that 514-nm pumping led to much stronger up-conversion, owing to

"Big Picture" opening →

Optical irradiation accompanied by spontaneous anti-Stokes emission can lead to cooling of matter, in a phenomenon known as laser cooling, or optical refrigeration, which was proposed by Pringsheim in 1929[1]. In gaseous matter, an extremely low temperature can be obtained in diluted atomic gases by Doppler cooling[2], and laser cooling of ultradense gas has been demonstrated by collisional redistribution of radiation[3]. In solid-state materials, laser cooling is achieved by the annihilation of phonons, which are quanta of lattice vibrations, during anti-Stokes luminescence. Since the first experimental demonstration in glasses doped with rare-earth metals[4], considerable progress has been made, particularly in ytterbium-doped glasses or crystals: recently a record was set of cooling to about 110 kelvin from the ambient temperature, surpassing the thermoelectric Peltier cooler[5,6]. It would be interesting to realize laser cooling in semiconductors, in which excitonic resonances dominate[7–9], rather than in systems doped with rare-earth metals, where atomic resonances dominate. However, so far no net cooling in semiconductors has been achieved despite much experimental[10–12] and theoretical[7–9,13,14] work, mainly on group-III–V gallium arsenide quantum wells. Here we report a net cooling by about 40 kelvin in a semiconductor using group-II–VI cadmium sulphide nanoribbons, or nanobelts, starting from 290 kelvin. We use a pump laser with a wavelength of 514 nanometres, and obtain an estimated cooling efficiency of about 1.3 per cent and an estimated cooling power of 180 microwatts. At 100 kelvin, 532-nm pumping leads to a net cooling of about 15 kelvin with a cooling efficiency of about 2.0 per cent. We attribute the net laser cooling in cadmium sulphide nanobelts to strong coupling between excitons and longitudinal optical phonons (LOPs), which allows the resonant annihilation of multiple LOPs in luminescence up-conversion processes, high external quantum efficiency and negligible background absorption. Our findings suggest that, alternatively, group-II–VI semiconductors with strong exciton–LOP coupling could be harnessed to achieve laser cooling and open the way to optical refrigeration based on semiconductors.

Background info; narrowing of focus to specific topic →

Optical irradiation accompanied by spontaneous anti-Stokes emission can lead to cooling of matter, in a phenomenon known as laser cooling, or optical refrigeration, which was proposed by Pringsheim in 1929[1]. In gaseous matter, an extremely low temperature can be obtained in diluted atomic gases by Doppler cooling[2], and laser cooling of ultradense gas has been demonstrated by collisional redistribution of radiation[3]. In solid-state materials, laser cooling is achieved by the annihilation of phonons, which are quanta of lattice vibrations, during anti-Stokes luminescence. Since the first experimental demonstration in glasses doped with rare-earth metals[4], considerable progress has been made, particularly in ytterbium-doped glasses or crystals: recently a record was set of cooling to about 110 kelvin from the ambient temperature, surpassing the thermoelectric Peltier cooler[5,6]. It would be interesting to realize laser cooling in semiconductors, in which excitonic resonances dominate[7–9], rather than in systems doped with rare-earth metals, where atomic resonances dominate. However, so far no net cooling in semiconductors has been achieved despite much experimental[10–12] and theoretical[7–9,13,14] work, mainly on group-III–V gallium arsenide quantum wells. Here we report a net cooling by about 40 kelvin in a semiconductor using group-II–VI cadmium sulphide nanoribbons, or nanobelts, starting from 290 kelvin. We use a pump laser with a wavelength of 514 nanometres, and obtain an estimated cooling efficiency of about 1.3 per cent and an estimated cooling power of 180 microwatts. At 100 kelvin, 532-nm pumping leads to a net cooling of about 15 kelvin with a cooling efficiency of about 2.0 per cent. We attribute the net laser cooling in cadmium sulphide nanobelts to strong coupling between excitons and longitudinal optical phonons (LOPs), which allows the resonant annihilation of multiple LOPs in luminescence up-conversion processes, high external quantum efficiency and negligible background absorption. Our findings suggest that, alternatively, group-II–VI semiconductors with strong exciton–LOP coupling could be harnessed to achieve laser cooling and open the way to optical refrigeration based on semiconductors.

Motivation for paper (or "straw man" statement): why the research in this paper is necessary →

Optical irradiation accompanied by spontaneous anti-Stokes emission can lead to cooling of matter, in a phenomenon known as laser cooling, or optical refrigeration, which was proposed by Pringsheim in 1929[1]. In gaseous matter, an extremely low temperature can be obtained in diluted atomic gases by Doppler cooling[2], and laser cooling of ultradense gas has been demonstrated by collisional redistribution of radiation[3]. In solid-state materials, laser cooling is achieved by the annihilation of phonons, which are quanta of lattice vibrations, during anti-Stokes luminescence. Since the first experimental demonstration in glasses doped with rare-earth metals[4], considerable progress has been made, particularly in ytterbium-doped glasses or crystals: recently a record was set of cooling to about 110 kelvin from the ambient temperature, surpassing the thermoelectric Peltier cooler[5,6]. It would be interesting to realize laser cooling in semiconductors, in which excitonic resonances dominate[7–9], rather than in systems doped with rare-earth metals, where atomic resonances dominate. However, so far no net cooling in semiconductors has been achieved despite much experimental[10–12] and theoretical[7–9,13,14] work, mainly on group-III–V gallium arsenide quantum wells. Here we report a net cooling by about 40 kelvin in a semiconductor using group-II–VI cadmium sulphide nanoribbons, or nanobelts, starting from 290 kelvin. We use a pump laser with a wavelength of 514 nanometres, and obtain an estimated cooling efficiency of about 1.3 per cent and an estimated cooling power of 180 microwatts. At 100 kelvin, 532-nm pumping leads to a net cooling of about 15 kelvin with a cooling efficiency of about 2.0 per cent. We attribute the net laser cooling in cadmium sulphide nanobelts to strong coupling between excitons and longitudinal optical phonons (LOPs), which allows the resonant annihilation of multiple LOPs in luminescence up-conversion processes, high external quantum efficiency and negligible background absorption. Our findings suggest that, alternatively, group-II–VI semiconductors with strong exciton–LOP coupling could be harnessed to achieve laser cooling and open the way to optical refrigeration based on semiconductors.

Optical irradiation accompanied by spontaneous anti-Stokes emission can lead to cooling of matter, in a phenomenon known as laser cooling, or optical refrigeration, which was proposed by Pringsheim in 1929[1]. In gaseous matter, an extremely low temperature can be obtained in diluted atomic gases by Doppler cooling[2], and laser cooling of ultradense gas has been demonstrated by collisional redistribution of radiation[3]. In solid-state materials, laser cooling is achieved by the annihilation of phonons, which are quanta of lattice vibrations, during anti-Stokes luminescence. Since the first experimental demonstration in glasses doped with rare-earth metals[4], considerable progress has been made, particularly in ytterbium-doped glasses or crystals: recently a record was set of cooling to about 110 kelvin from the ambient temperature, surpassing the thermoelectric Peltier cooler[5,6]. It would be interesting to realize laser cooling in semiconductors, in which excitonic resonances dominate[7–9], rather than in systems doped with rare-earth metals, where atomic resonances dominate. However, so far no net cooling in semiconductors has been achieved despite much experimental[10–12] and theoretical[7–9,13,14] work, mainly on group-III–V gallium arsenide quantum wells. Here we report a net cooling by about 40 kelvin in a semiconductor using group-II–VI cadmium sulphide nanoribbons, or nanobelts, starting from 290 kelvin. We use a pump laser with a wavelength of 514 nanometres, and obtain an estimated cooling efficiency of about 1.3 per cent and an estimated cooling power of 180 microwatts. At 100 kelvin, 532-nm pumping leads to a net cooling of about 15 kelvin with a cooling efficiency of about 2.0 per cent. We attribute the net laser cooling in cadmium sulphide nanobelts to strong coupling between excitons and longitudinal optical phonons (LOPs), which allows the resonant annihilation of multiple LOPs in luminescence up-conversion processes, high external quantum efficiency and negligible background absorption. Our findings suggest that, alternatively, group-II–VI semiconductors with strong exciton–LOP coupling could be harnessed to achieve laser cooling and open the way to optical refrigeration based on semiconductors.

Preview of key results in this paper

Informal (ungraded) homework assignment

Using your journal club and/or referee report paper selection:

1. Read the abstract of your paper carefully, and see if it has the Motivation, Methods, Results, and Significance structure we discussed today. If not, assess whether the abstract could have been improved with this structure.

2. Read the introduction of your paper carefully, and see if it has the structure discussed today: "Big Picture" Motivation, Background Information/Narrowing Focus, Motivation for Research, and Preview of Key Results. If not, assess whether the introduction could have been improved with this structure.

Summary: Crafting an Accessible Scientific Paper

Make sure you have a coherent story to tell:
writing a draft abstract and introduction can help identify and refine your story.

Create a logical flow to the story you're telling:
start with a detailed outline! Make use of paragraphs with a clear topic sentence and one idea per paragraph.

Avoid disruptions to accessibility in your narrative:
keep sentences short, avoid acronyms and unfamiliar words and scientific terms, avoid colloquial phrases, avoid ambiguous pronouns.

Questions? slcooper@Illinois.edu